Available online at www.sciencedirect.com
SCIENCE DIRECT®
Journal of Crystal Growth 286 (2006) 284–287
JOURNAL OF CRYSTAL GROWTH
www.elsevier.com/locate/jcrysgro

In situ observations in the melt growth of $Pb_5Ge_3O_{11}$ crystals

Y. Hong[a], W.Q. Jin[a,*], X.H. Pan[a], X.J. Wu[a], J.Y. Xu[a], Y. Shinichi[b]

[a]*Shanghai Institute of Ceramics, Chinese Academy of Science, 200050 Shanghai, PR China*
[b]*Space Utilization Research Center, Office of Space Utilization System, JAXA, 2-2-1, Sengen, Tsukuba, Ibaraki 305, Japan*

Received 23 March 2005; accepted 15 August 2005
Available online 28 November 2005
Communicated by T. Hibiya

Abstract

The interface motion during the growth process of $Pb_5Ge_3O_{11}$ from the melt is visualized in an in situ observation system. The formation of the striation aggregation is observed, and the rates of the interface motion R_{im} are measured. It turns out that there are sharp changes in the growth rate during the formation of the striation aggregation. It has been found that the typical fluctuation in the rates can be associated with the kinetics and transport mixed control during the crystal growth. The non-uniform composition normal to the interface gives rise to the striation aggregation. Of particular importance in the investigation are the typical interfacial melt flows from the corners to the center of the interface observed in the experiments. The relation between the rates of this interfacial melt flow R_{if} and the time t is also provided showing that the change of supersaturation adjacent to the interface gives rise to the interfacial melt flow.

PACS: 81.10; 61.72

Keywords: A1. Defects; A1. Mass transfer; A1. Growth models

1. Introduction

Owing to its novel ferroelectric properties and reversible optical activity, lead germanate $Pb_5Ge_3O_{11}$ (PGO) has attracted much interest in the past years [1–4]. Thus, PGO single crystals are becoming a promising basis to fabricate pyroelectric detectors [5]. The optical activity of PGO can be used in the fields of information storage and light signal processing [2–7].

However, growth striations, which are usually found in crystals grown from both the melt and from solutions, tremendously deteriorate the quality of PGO crystals. In a previous study on PGO growth using the Bridgman method, the uniformity of the crystals was found to be greatly affected by the fluctuation of growth rate, causing the occurrence of striations which mark the growth interface [7]. But, so far little is known about the direct connection between the striation and the growth rate in PGO crystal growth, mainly because it is technically difficult to visualize and measure the interface growth rate in the high-temperature environment.

Concerning the formation of striations in melt as well as in solution crystal growth, some important works had been carried out in order to get an overall knowledge of this subject [8–14]. However, the growth rates were mostly determined by comparing the central distances of the respective faces at the beginning and the end of the growth process in these studies. Thus, they just gave a rather integrating value. A more detailed analysis of the growth rate variation with the formation of the striation in the high-temperature oxide melt has not yet been made, although it is of great importance to direct the industrial oxide crystal growth, as well as with respect to its theoretically significance for studying the growth mechanism.

In our observation system, the whole process of PGO melt crystal growth including the formation of the striation aggregation can be visualized, which enables us to carry out a detailed study on the connection between the rate change and the striation formation. We thus emphasize the experimental report on the connection between the

*Corresponding author. Tel.: +86 21 52412502; fax: +86 21 52413903.
E-mail address: wqjin@sunm.shcnc.ac.cn (W.Q. Jin).

0022-0248/$ - see front matter © 2005 Elsevier B.V. All rights reserved.
doi:10.1016/j.jcrysgro.2005.08.061

interface motion rate and the formation of the striation, which is their aggregation in this work. Even more interesting is the typical interfacial melt flow observed in the experiments.

2. Experimental procedure

In the experiments reported here, the space high-temperature in situ observation instrument 'SHITISOI' is adopted, as explained elsewhere [15,16]. The test section comprised of a heating chamber and a loop-shaped Pt wire heater. As shown in Fig. 1(a) (position "a"), the Pt wire ($\Phi = 0.2$ mm) is supposed to heat and suspend the melt during the in situ observation experiment. A Pt–10% Rh thermocouple ($\Phi = 0.08$ mm) is used to measure the temperature of the loop (position "b" in Fig. 1(a)). The diameter of the loop is about 2.0 mm. A V-type electrode is used to defend the loop-shaped heater from deformation. Power is applied to both sides of the wire (positions "c" and "d" in Fig. 1(a)). Temperature control was achieved by changing the voltage of the power applied on the loop. To observe the whole crystal growth, the sample was melted, and the amount of test melt was precisely controlled until a thin translucent flat film was obtained. Then, the melt was quenched and numerous grains were seeded, but only one grain was chosen and allowed to grow while the others are melted off. Schlieren technique coupled with differential interference microscope are applied to visualize the whole process of crystal growth, and video from the microscope (through CCD) is recorded by a computer, which enables us to analyze the video later.

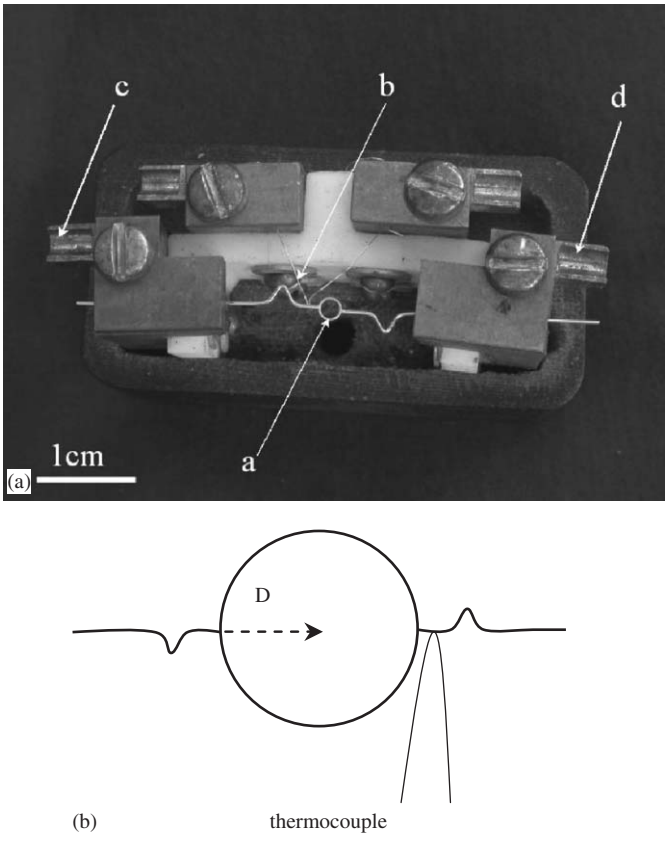

Fig. 1. (a) Photograph of the heating chamber; (b) schematic diagram of the experimental test section (for details see text).

3. Results and discussion

The temperature distribution along the melt-free surface is an important source of information because it is directly related to the rate of crystal growth. The radial temperature distribution was measured by a newly developed non-contact method [17]. Fig. 2 shows the radial temperature distribution in the melt. It should be noted that "D" in x-coordinate in Fig. 2 means the radial distance from the periphery of the loop. It can be seen that the temperature of the melt adjacent to the periphery of the loop is higher than in its center area, which is due to natural cooling by air. It is to be noted that the crystal growth is carried out in the center area in order to minimize the influence by the radial temperature difference.

The formation of the striation aggregation has been observed in experiments and the connection between the interface motion rate R_{im} and the striation aggregation has also been built up, which is described as follows.

The rates R_{im} are calculated by dividing the growth distances by the respective growth times. The growth distances are measured from the seeds to the liquid–solid interface of the crystal. As it is shown in Fig. 3(a), the growth striation aggregations (1)–(3) decorate the respective position of the growing interface. The rate of interface motion is observed to evidently undergo a positive and a negative pulse when the striation aggregation happens. As mentioned above, R_{im} can be determined through a computer analysis of the video recorded. From this analysis, R_{im} turns out to fluctuate with the formation of the striation aggregation. Fig. 3(b) shows the variation of the rates R_{im} as a function of time t. It is noted that the

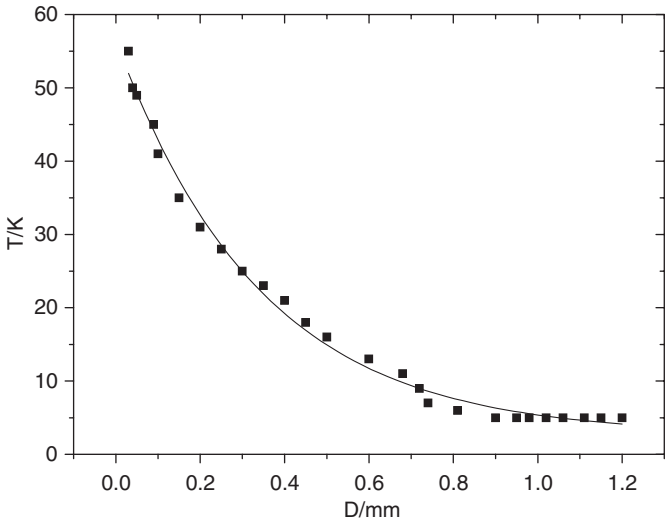

Fig. 2. Radial temperature difference in the melt of the loop-shaped heater.

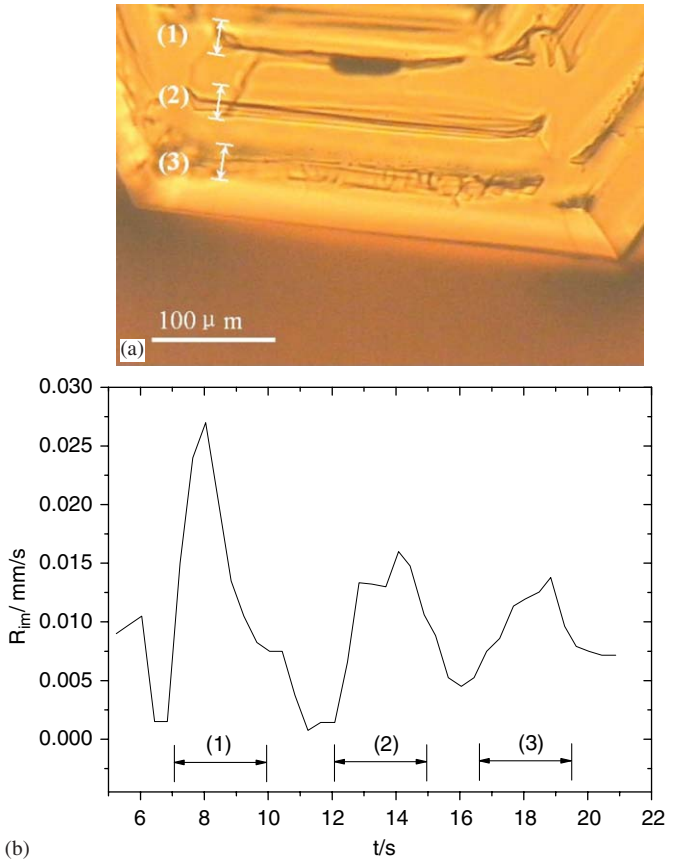

Fig. 3. (a) Striation aggregations (1)–(3) in the PGO crystal growth from melt. (top view); (b) changes of the rates of the interface motion R_{im} as a function of time t.

marked time intervals (1)–(3) in Fig. 3(b) are corresponding to the time intervals when the striation aggregations (1)–(3) occur in Fig. 3(a), respectively. Fig. 3(b) clearly shows that the rate of interface motion increases sharply to the maximum 0.027 mm/s when the striation aggregation (1) in Fig. 3(a) happens, and then the rate R_{im} decreases suddenly. After that, the flat interface motion is achieved again, but its rate keeps on decreasing until it reaches the lowest value (0.002 mm/s). As shown in Fig. 3(a), further striation aggregations (2) and (3) occur. Correspondingly, the rate R_{im} alternates appropriately. However, the maximum and minimum rates differ when comparing the observed striation aggregations. As shown in Fig. 3a, the flat interface motion dominates the interval between (1) and (2), and between (2) and (3).

The typical fluctuation in the rate R_{im} should be associated with the kinetics and transport control during the crystal growth [8,9]. If the interfacial concentration approaches the bulk concentration, the growth proceeds under pure kinetics control, whereas it is transport-controlled when it approaches the equilibrium concentration. The system can be assumed to be stable only if one mechanism is responsible for controlling the growth. For mixed control as it occurs in PGO crystal growth, however, the system is unstable, which gives rise to the fluctuant rate in Fig. 3(b).

The formation of the striation aggregation could be interpreted as follows. The fluctuation in the growth rate leads to an alternating effective segregation coefficient. As a result, the composition becomes non-uniform normal to the interface, which can be manifested by the SEM-EDS testing results in the striation aggregation areas and the other areas without striation. It turns out that PbO concentration in the areas with striations is 74.21 wt%, which is smaller than 75.76 wt% in the areas without striations. It is the inhomogeneity in the composition that can be seen as the striation aggregation.

Furthermore, there is a typical interfacial melt flow parallel to the interface accompanying the formation of the striation aggregation, observed in Fig. 3(a). To study the phenomenon, another experiment concerning the interfacial melt flows from the corners to the center of the interface had been carried out. Fig. 4a shows three momentary pictures of the interfacial melt flows. The pictures show the interfacial melt flow starting from the corner (position A in Fig. 4(a)), its position after 0.35 s (position B) and after 0.85 s (position C). The opposite interfacial melt flows from the two corners will encounter after that in Fig. 4(c). Then, another period of the interfacial melt flow adjacent to the formed striation aggregation occurs, and forms another striation aggregation. The width of the interfacial melt flow is about 20 μm.

The corresponding rates of the interfacial melt flow R_{if} in positions A, B and C are evidently shown in Fig. 4(d). The values are calculated as a quotient of the distance traveled by the interfacial melt flow and the corresponding time

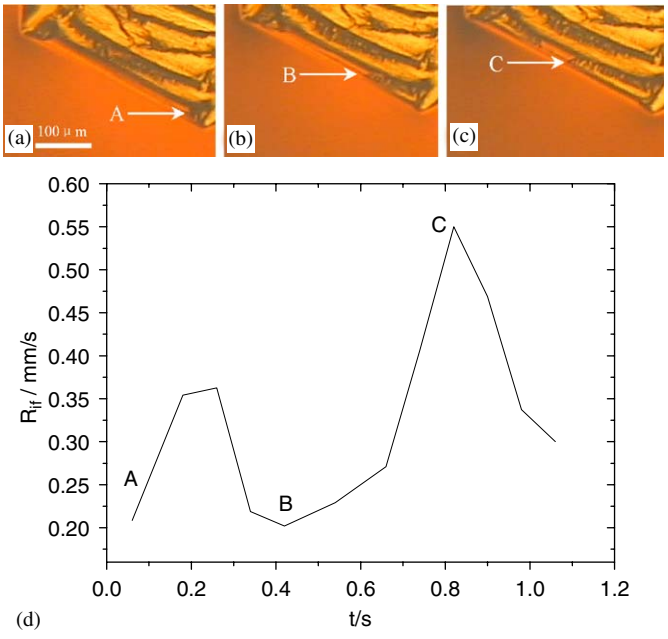

Fig. 4. Interfacial melt flow from the corner to the center of the interface (top view): (a) position A—$t = 0.08$ s, $R_{if} = 2.33$ mm/s; (b) position B—$t = 0.40$ s, $R_{if} = 2.06$ mm/s; (c) position C—$t = 0.82$ s, $R_{if} = 5.48$ mm/s; (d) Time dependence of the rates of interfacial melt flow R_{if}.

interval. The distance is measured from the corner to the front of the interfacial melt flow. The rate R_{if} exhibits two periods of increase and decrease of its value.

This dependence of the rate on time can be understood in terms of the change of the concentration of PbO adjacent to the interface. It is assumed that the concentration gradient along the interface leads to the solution flows parallel to the line from the corners to the center. At the beginning, the supersaturation near the corners rises and causes an increase in the rate of interfacial melt flow R_{if}. However, the rate decreases with the solute loss (Fig. 4(d)). Then, the negative concentration gradient in the melt near the corners is compensated for due to a convective transport mechanism. So, the supersaturation around the corners would speed-up the interfacial melt flow again. As shown in Fig. 4(d), the rate of interfacial melt flow would increase sharply again until the encounter of the two opposite interfacial melt flows, which can be associated with the second increase and decrease in the rate R_{if}.

4. Conclusion

The connection between the rates of interface motion and formation of the striation aggregation had been built up. In the in situ observation system, the formation of the striation aggregation was visualized and the interface motion rates R_{im} were measured, and turned out to change with the formation of the striation aggregation. It was pointed out that there was a competition between the transport and the kinetics in the process of the interface motion, and the growth rate R_{im} tended to fluctuate when the interface motion was under the mixed control of the kinetics effect and the transport effect. The fluctuation in the growth rate gave rise to a fluctuant effective segregation coefficient, and the inhomogeneity of the PbO concentration caused the striation aggregation. The typical opposite interfacial melt flows from the corners to the center of the interface were visualized in the experiments. The rate of the interfacial melt flow R_{if} was also found to change when it traveled along the interface, which was explained to occur due to the changes of supersaturation along the interface.

Acknowledgements

This work has been supported by the National Natural Science Foundation of China under Grant no. 50331040, and the Innovation Funds from the Chinese Academy of Sciences (KJCXZ-SW-105-03).

References

[1] H. Iwasaki, K. Sugii, T. Yamada, N. Niizeki, Appl. Phys. Lett. 18 (1971) 444.
[2] S. Nanamatsu, H. Sugiyama, K. Dol, Y. Konda, J. Phys. Soc. Jpn. 31 (1971) 616.
[3] H. Iwasaki, K. Sugii, Appl. Phys. Lett. 19 (1971) 92.
[4] J.P. Dougherty, E. Sawaguchi, L.E. Cross, Appl. Phys. Lett. 20 (1972) 364.
[5] N.K. Misra, R. Sati, R.N.P. Choudhary, Mater. Lett. 27 (1996) 95.
[6] R.E. Newnham, R.W. Wolfe, C.N.W. Darlington, J. Solid State Chem. 6 (1973) 378.
[7] X.J. Wu, J.Y. Xu, J.Z. Xiao, A.H. Wu, W.Q. Jin, J. Crystal Growth 263 (2004) 208.
[8] C.J. Allegre, A. Provost, C. Jaupart, Nature 294 (1981) 223.
[9] L.A. Monaco, F. Rosenberger, J. Crystal Growth 168 (1993) 1.
[10] A.A. Chernov, J. Crystal Growth 118 (1992) 33.
[11] P.G. Vekilov, J.I.D. Alexander, F. Rosenberger, Phys. Rev. E 54 (1996) 6650.
[12] S.Yu. Potapenko, J. Crystal Growth 147 (1995) 233.
[13] R.U. Barz, M. Grassl, P. Gille, J. Crystal Growth 237 (2002) 843.
[14] T. Kamei, T. Inoue, S. Yanagiya, A. Mori, J. Crystal Growth 243 (2002) 517.
[15] W.Q. Jin, Z.H. Liu, Z.L. Pan, F. Bao, X.T. Xia, M.J. Zhu, Micrograv. Sci. Technol. (1997) 194.
[16] W.Q. Jin, S. Yoda, Y.F. Jiang, Z.L. Pan, X.A. Liang, Chin. Phys. Lett. 18 (2001) 435.
[17] X.A. Liang, W.Q. Jin, Z.H. Liu, Z.L. Pan, Prog. Cryst. Growth Mater. Characterist. 40 (2000) 301.